Signal analysis of impulse response functions in MR- and CT-measurements of cerebral blood flow

Evelyn Rost[a,c], Ralf Geske[b] and Michael Baake[a]

(a) Fakultät für Mathematik, Univ. Bielefeld, Box 10 01 31, 33501 Bielefeld, Germany

(b) Institut für klinische Physik und Biomedizintechnik, Dietrich Bonhoeffer Klinikum Neubrandenburg, Allendestr. 30, 17036 Neubrandenburg, Germany

(c) Institut für Mathematik und Informatik, Univ. Greifswald, Jahnstr. 15 a, 17487 Greifswald, Germany

Abstract

The impulse response function (IRF) of a localized bolus in cerebral blood flow codes important information on the tissue type. It is indirectly accessible both from MR- and CT-imaging methods, at least in principle. In practice, however, noise and limited signal resolution render standard deconvolution techniques almost useless. Parametric signal descriptions look more promising, and it is the aim of this contribution to develop some improvements along this line.

Key Words: blood flow, tissue determination, parametric fits,
Fourier transform, MR- and CT-imaging

1   Introduction

The detailed knowledge of blood circulation in the brain is beyond doubt an important diagnostic tool. Among other aspects, it admits the detection and a partial characterization of cerebro vascular and tumorous diseases. Apart from the relative cerebral blood volume, the mean transit time is a basic diagnostic parameter. For its determination, the so-called impulse response function (sometimes also called impulse residue function) [2, 17]

1

of the tissue is needed, which, unfortunately, is not accessible to direct measurement. Previous contributions consistently showed various deficiencies in regard to its determination, especially if diffusive tissue areas were involved.

The aim of this contribution is to analyze such deficiencies from a more mathematical point of view and to point out a method that is practically feasible. Both MR and CT perfusion measurements are included here.

First, we notice that the determination of the impulse response function of tissue by a direct deconvolution from the arterial and tissue signal does not seem to be possible in a reliable way. A solution is then suggested on the basis of a parametric fit. In the case of a disturbed blood brain barrier, it is shown that an estimation of the mean transit time is possible also with CT perfusion measurements, although a CT measurement is short in comparison to an MR measurement since CT measurement is time limited due to radiation exposure.

The paper is organized as follows. First, we briefly summarize the deconvolution methods used, and their common deficiencies in our practical situation. We continue with a more detailed discussion of parametric fits. Here, we discard the so-called double gamma fit, because it can be shown to lead to inconsistent results. Nevertheless, a closely related pair of parametric functions works rather well and is suggested as an alternative.

We describe first steps towards the parametric treatment of data from defective tissue, and close with the suggestion of a quantity to distinguish intact from disturbed blood brain barrier. This is the standard deviation of the IRF and can replace the mean transit time. It is directly accessible even without a parametric fit, both for MR and CT data.

2   Shortcomings of convolution techniques

Three numerical deconvolution methods were analyzed in [13]. They are deconvolution by

1. Fourier transform

2. the method of moments

3. functional calculus.

These methods were first tested by realistic, but simulated data without noise. They provide acceptable and comparable results if the sampling rate is sufficiently high (which roughly means some five to ten sampling points per relevant interval of time). Let us explain the deconvolution approach in some more detail.

1. The deconvolution by Fourier transform uses the convolution theorem [6, p. 110], so that one gets

$$g = \left(\frac{(f * g)\hat{}}{f\hat{}} \right)\check{},$$ (1)

where $(.)\hat{}$ denotes the Fourier transform and $(.)\check{}$ the corresponding inverse transform. One principle problem is the following. Whenever the Fourier transform of f and g are equal in a certain interval including zero, and the Fourier transform of f is zero outside this interval, then $(f * f)\hat{} = (f * g)\hat{}$. In general, it is thus not correct that $f * g_1 = f * g_2$ implies $g_1 = g_2$. This means that the deconvolution is not well defined in general, compare [12, Ch. 7] for a general discussion. Fortunately, in our present context, this aspect does not play a major role. Another numerical problem, which is more important in our case, can emerge from (approximate) zeros of the denominator of (1). It is obvious that the zeros of $f\hat{}$ form a subset of those of $(f * g)\hat{}$, and that (1) is always well defined from the theoretical point of view. However, since the Fourier transforms have to be determined numerically from discrete data, it can occur that the approximation of $f\hat{}$ features zeros where that of $(f * g)\hat{}$ does not. This makes expression (1) undefined or leads to undesirable fluctuations. Finally, the numerical data for f and for $f * g$ show similar noise level. In theory, $f * g$ should be the smoother signal though, and a violation can (and actually does) lead to numerical sensitivity of the (discrete) inverse transform.

2. If the function g (or a good approximation of it) is known in some parametric form, the unknown parameters can be determined by the method of moments. To this end, we need the following relation [13]: If f and g are non-negative, suitably integrable, normalized functions, then

$$\langle X^n \rangle_{f*g} = \sum_{k=0}^{n} \binom{n}{k} \langle X^{n-k} \rangle_g \langle X^k \rangle_f ,$$ (2)

where $\langle X^n \rangle_h := \int x^n h(x) dx$ is the n-th moment of h. In particular, we assume that all these moments exist, which is very reasonable in our context.

Assume that it is possible to describe g by m parameters. In this case, all moments up to order $(m - 1)$ of f and $f * g$ are needed to create a complete set of equations by means of (2). In our case, the functions f and $f * g$ are non-negative, but not normalized (this can be mended by dividing by their respective integrals). Since, however, the moments have to be calculated numerically, they will show decreasing accuracy with increasing m. Consequently, this approach is only useful for situations with a small number of parameters.

3. Deconvolution by the functional calculus is a less well known, but rather interesting method. It provides a kind of inverse formula to determine the function g if f and $f * g$ are given. This does not work for any arbitrary function f but f has to be a special type of function. In principle, the method applies to our situation, which had been overlooked

in previous attempts. The following example shall illustrate this method. If

$$f(t) = \begin{cases} te^{-t}, & t \geq 0, \\ 0, & \text{otherwise,} \end{cases} \tag{3}$$

the equation $(f * g)(t) = \int_{\mathbb{R}} f(t - x)g(x)dx$ is inverted by

$$g(t) = (1 + D)^2 (f * g)(t), \tag{4}$$

where $D = \frac{d}{dt}$ is the derivation operator. This means that g can be calculated by the first and the second derivative of $f * g$, if f is according to (3). Further examples, and a systematic theory, can be found in [11]. Unfortunately, derivatives play a major role, and, with increasing complexity of the convolution kernel, the derivatives required are of higher and higher order. Since the actual data are discrete values, the derivatives have to be calculated numerically. Hence, this method is suitable only to a limited extent due to numerical sensitivity.

As a common problem to all three methods, the sampling rate of about one point per second of an MR and a CT scanner is too coarse. This is demonstrated by the following simple example. The function $f(t) = te^{-t}$, $t \geq 0$, was convolved with a rectangular signal g of width 3 and height 0.2 (hence not normalized) to obtain $f * g$. Then, the particular functions were sampled at different rates. The results of deconvolution by the three methods are shown in Figure 1, whereas the dashed rectangle is the original function g for comparison.

In comparison to this illustrative example, our real world case corresponds to the leftmost column in Figure 1, i.e., to a clearly insufficient resolution. Note that the same qualitative picture would emerge for other signal types as well, not just for rectangular g.

Additionally, the real data are superimposed by noise. From a careful inspection of our sample data, we estimate that noise and measurement errors together result in fluctuations of five to ten percent on average. It is well known that numerical deconvolution processes can be very sensitive to noise. Therefore, it is preferable to describe the measured data by functions, e.g., by means of a parametric ansatz followed by a least squares fit. This requires an adequate approach.

3   Inadequacy of the double gamma fit

Fitting the data by gamma densities (in the literature mostly called gamma variate functions [3, 15]) seems to be an adequate approach. Especially the measured arterial signals can be described this way. But sometimes both arterial and tissue signal were displayed
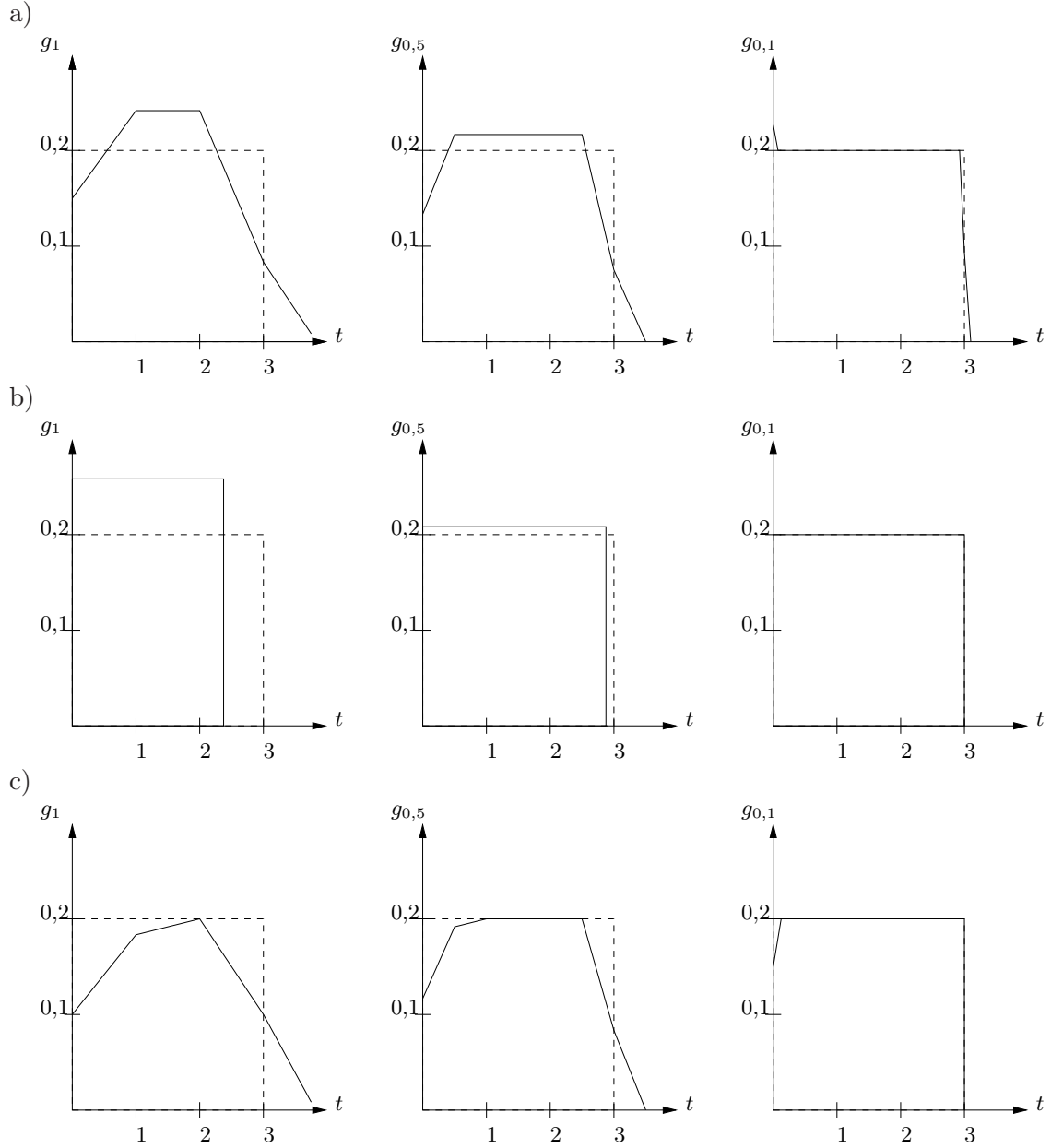
Figure 1: *Results of deconvolution by a) Fourier transform b) the method of moments and c) the functional calculus in dependence on the sampling rate. The latter is one point (left), two points (center) and ten points (right) per relevant interval of time (which is 1 in this case). For better illustration, the discrete sample points are successively connected by straight lines without additional interpolation. Note, that the function g is not normalized.*

by gamma densities [16, 17]. In this section, we want to show that such a double gamma fit is not reasonable.

For simplicity, we formulate the situation in terms of probability theory. The actual signals are described by non-negative functions that need not be normalized. However, the normalization constants play no role here (one can simply divide by them to get normalized signals), so that we can profit from the standard tools of probability theory.

If f is an integrable non-negative function,

$$\phi(t) = \int_{\mathbb{R}} e^{itx} f(x) dx \tag{5}$$

is the (inverse) Fourier transform of f. If f is a probability density, ϕ is called its *characteristic function*, see [14] for details. In the case of $f = f_{\lambda,\alpha}$ being a (normalized) gamma density, i.e.,

$$f_{\lambda,\alpha}(x) = \begin{cases} 0, & x < 0, \\ \frac{\lambda^\alpha}{\Gamma(\alpha)} x^{\alpha-1} e^{-\lambda x}, & x \geq 0, \end{cases} \tag{6}$$

with $\lambda > 0$, $\alpha > 1$ and $\Gamma(\alpha) = \int_0^\infty x^{\alpha-1} e^{-x} dx$, the characteristic function is [14, p. 343]

$$\phi_{\lambda,\alpha}(t) = \left(\frac{\lambda}{\lambda - it} \right)^\alpha, \quad \text{with } t \in \mathbb{R}, \tag{7}$$

which can be calculated with elementary methods from complex analysis.

Starting from two gamma densities, we consider the convolution $f_{\lambda,\alpha} * g = f_{\gamma,\nu}$. (In doing so, $f_{\lambda,\alpha}$ corresponds to the measured arterial signal and $f_{\gamma,\nu}$ to the tissue signal, whereas g is the IRF wanted, up to a multiplicative factor). By means of the convolution theorem and the characteristic function of the gamma density, one gets the characteristic function of g as

$$\phi_g(t) = \frac{\nu^\gamma (\lambda - it)^\alpha}{(\nu - it)^\gamma \lambda^\alpha} =: h(t). \tag{8}$$

The central question now is whether h is the characteristic function of a probability density. An answer is given by the Bochner-Khintchine theorem which states that a continuous function $\varphi(t)$, $t \in \mathbb{R}$, with $\varphi(0) = 1$ is the characteristic function of a probability measure if and only if it is positive definite, see the appendix for details.

The violation of some elementary properties of positive definite functions in this case already implies that h is not positive definite in general. Fitting the data by gamma densities provides parameters in a region where property (3) of the appendix is violated, see [13] for details. Consequently, h is not a characteristic function and therefore g is not a probability density. This, in turn, means that g takes negative values which cannot be interpreted in our context. Consequently, the sometimes used double gamma fit is not consistent in this context and should be avoided.

4   An alternative approach

Let us look for an alternative. It is reasonable (and also rather plausible) to assume the IRF itself to be gamma distributed. In this case, we can calculate the shape of the tissue signal if the arterial signal is still described by a gamma density. We have to determine $f * g$ provided that $f = f_{\lambda,\alpha}$ and $g = g_{\mu,\beta}$ according to (6). Once again, by means of the convolution theorem and the characteristic function of the gamma density, one now finds

$$\phi_{f*g}(t) = \left(\frac{\lambda}{\lambda - it}\right)^{\alpha} \left(\frac{\mu}{\mu - it}\right)^{\beta} = \lambda^{\alpha}\mu^{\beta}(\lambda - it)^{-\alpha}(\mu - it)^{-\beta} , \tag{9}$$

with $\phi_{f*g}(0) = 1$. The corresponding inverse transform reads [10, Ch. 3.2]

$$\begin{aligned}
(f * g)(x) &= \lambda^{\alpha}\mu^{\beta} \frac{e^{-\lambda x}x^{\alpha+\beta-1}}{\Gamma(\alpha+\beta)} {}_1F_1[\beta; \alpha+\beta; (\lambda-\mu)x] \\
&= \lambda^{\alpha}\mu^{\beta} \frac{e^{-\mu x}x^{\alpha+\beta-1}}{\Gamma(\alpha+\beta)} {}_1F_1[\alpha; \alpha+\beta; (\mu-\lambda)x]
\end{aligned} \tag{10}$$

for $x \geq 0$ and $(f * g)(x) = 0$ otherwise, where ${}_1F_1$ is the confluent hypergeometric function [1, Ch. 13] with

$$ {}_1F_1(a; b; z) := \sum_{k=0}^{\infty} \frac{(a)_k}{(b)_k} \frac{z^k}{k!} = 1 + \frac{az}{b} + \frac{a(a+1)}{b(b+1)} \frac{z^2}{2!} + \dots , $$

whereas $(c)_k := c(c+1) \cdot \dots \cdot (c+k-1)$ is the Pochhammer symbol. The normalization of the inverse transform is chosen such that $(f * g)(x)$ is indeed a normalized probability density, i.e., $(f * g)(x) \geq 0$ together with $\int_{\mathbb{R}_+} (f * g)(x)dx = 1$.

The two formulations of (10) are equal by Kummer's functional equation for ${}_1F_1$, see [1, Eq. 13.1.27]. For $\lambda > \mu$ (resp. $\lambda < \mu$) the first (resp. the second) version immediately shows the non-negativity of $(f * g)(x)$. For $\lambda = \mu$, $f * g$ is the density of a gamma distribution, in line with the convolution semigroup property $(f_{\lambda,\alpha} * f_{\lambda,\beta})(x) = f_{\lambda,\alpha+\beta}(x)$ for gamma densities with the same parameter λ, compare [9].

The question is now whether the tissue signal can be described by the expression in (10). An example (compare with Figure 2) shows that the fit is rather convincing, so that this ansatz is phenomenologically sound. Of course, it remains an interesting open question at this point whether further corroboration, e.g., by microscopic modelling, is possible.

The function in Eq. (10) fits the tissue signal at least as well as a gamma density would do. But in contrast to the latter, we no longer encounter problems with negative values of the IRF.

Note, however, that this approach can only be used for tissue with an intact blood brain barrier because the fit separates the recirculation from the real signal. Tissue with a defective blood brain barrier, such as a brain tumor, has to be considered separately because recirculation is superimposed by diffusion.
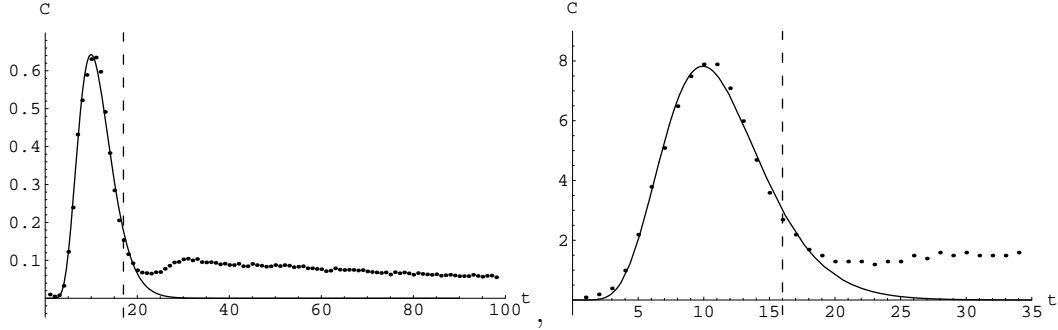
Figure 2: *Parametric fit of the tissue signal measured by an MR scanner (top) and a CT scanner (bottom), with the function from Eq. (10), up to an additional normalization factor. All points to the left of the dashed vertical line were used for the fit.*

4.1   Tissue with defective blood brain barrier

The measured signal of a tissue with a permeable blood brain barrier (e.g., brain tumor) consists of a diffusive and a perfusive part [5, 8]. The idea here is to split up these parts and deconvolve them separately. This way, additional features of the different contributions can be detected and displayed more clearly.

After injection of the contrast medium, most of these molecules remain in the intravascular space during their transit through the vascular network. However, a small portion diffuses into the extravascular space and then back into the intravascular space due to the defective blood brain barrier. Because diffusion is much slower than perfusion, contrast medium molecules still diffuse into the extravascular space during recirculation [5, 8, 15].

To our knowledge, there is no theoretical derivation known to describe the diffusive part in detail, wherefore a phenomenological approach is necessary and appropriate. The function

$$f(t) = \begin{cases} 0, & t < 0, \\ at^b e^{-ct^d}, & t \geq 0, \end{cases} \tag{11}$$

with $a > 0$, $b \geq 1$, $c > 0$ and $d > 0$ unknown parameters, seems to be applicable to capture the diffusion part parametrically, see Figure 3.

The perfusive part can be obtained approximately by subtraction of the diffusion part from the original signal (compare with Figure 4 top). Figure 4 bottom shows that (10) leads to a fit of acceptable quality. This means that the method introduced above can also be applied to determine the IRF of the perfusion. In this case, the IRF is a gamma density with the associated parameters from the fit.

It remains to consider the diffusive part. We did not find an explicit and practically useful expression for the IRF, so that we employed a numerical deconvolution technique (e.g., by Fourier transform). This, in contrast to above, does not pose a problem because both signals required are now available in parametrized form, and because the non-uniqueness
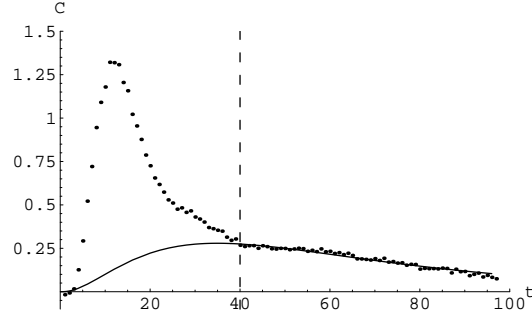
8

Figure 3: *The function $f(t) = at^b e^{-ct^d}$ as a parametric fit for the diffusive part. All points to the right of the dashed vertical line were used to determine the associated parameters.*
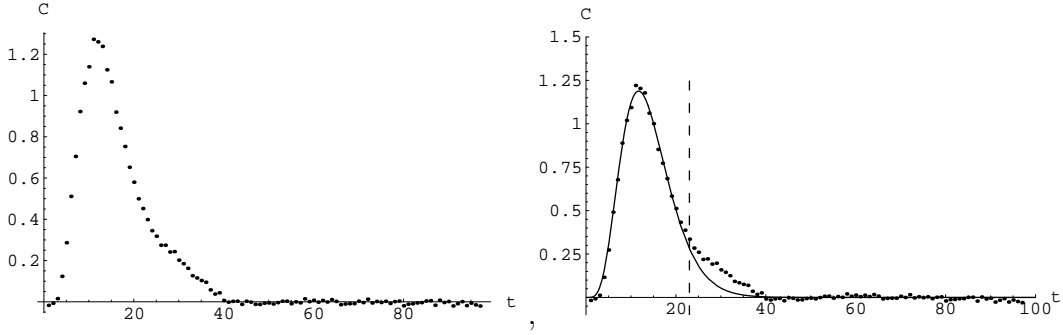

Figure 4: *Perfusion after subtraction of the diffusive part (top) and Eq. (10) as an adequate fit of the perfusion (bottom). All points to the left of the dashed line were used in this fit. The few points to the right not fitted by (10) are the remainder of recirculation.*

problem does not show up. Now, one can put the IRFs together to obtain the IRF of tissue with a permeable blood brain barrier. Figure 5 shows the IRFs for the different tissue types. On the top, the IRF for tissue with an intact blood brain barrier is shown, and the IRF for tissue with a defective blood brain barrier on the bottom.
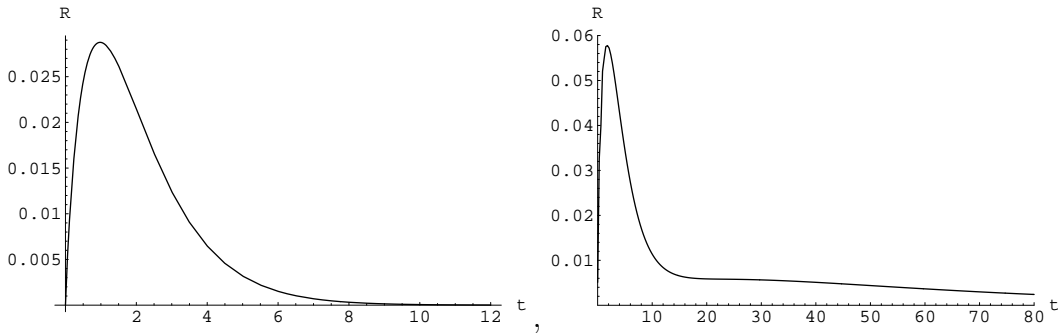

Figure 5: *The IRF for tissue with an intact blood brain barrier (top) and a defective blood brain barrier (bottom). Note the different scale on the time axis for comparison.*

9

4.2 Diagnostic parameters

So far, the *area to height relation* has been used to determine the mean transit time (MTT) [7, 17]. There, the area under the curve of the IRF is divided by the maximum of the IRF, i.e.,

$$MTT = \frac{\int R(t)dt}{R_{max}}, \tag{12}$$

if the IRF is denoted by R. However, this approach is only applicable for tissue with an intact blood brain barrier under the simplifying (and somewhat unrealistic) assumption that the IRF is a pulse of rectangular shape. By application of this formula to tissue with a permeable blood brain barrier, a rather unrealistic and unreliable estimate of the mean transit time is obtained. For characterizing and possibly detecting a brain tumor, a more reliable quantity is required.

The standard deviation of the IRF appears to be an adequate measure for the mean transit time. To expand on this suggestion, let f be a non-negative signal with a compact support. If $N = \int_{\mathbb{R}} f(t)dt$ is the normalization constant,

$$m_f := \frac{1}{N} \int_{\mathbb{R}} tf(t)dt \tag{13}$$

is the signal mean and

$$\sigma_f = \sqrt{\frac{1}{N} \int_{\mathbb{R}} (t - m_f)^2 f(t)\, dt} = \sqrt{\frac{1}{N} \int_{\mathbb{R}} t^2 f(t)dt - m_f^2} \tag{14}$$

is its standard deviation.

The standard deviation features the correct dimension, namely time, and does not change if the entire signal is shifted along the time axis. More importantly, its definition is independent of the shape of the IRF in the sense that it does not require any specific assumptions on the signal form. Consequently, it is applicable to the different tissue types.

In the case of the IRF being a non-normalized gamma density, there is an asymptotically linear relation between the mean transit time, computed by the area to height formula, and the standard deviation of the IRF. Thus, it is no big deal to replace the traditional formula by the standard deviation, because one calculates nothing much different in this case.

The theoretical relation can be derived as follows. Let the IRF again be denoted by R and assume that it is a non-normalized gamma density with parameters b, β and μ, i.e.,

$$R(t) = \begin{cases} b\frac{\mu^{\beta}}{\Gamma(\beta)} t^{\beta-1} e^{-\mu t}, & t \geq 0 \\ 0, & \text{otherwise.} \end{cases} \tag{15}$$

The standard deviation reads $\sigma_\Gamma = \frac{\sqrt{\beta}}{\mu}$, the area under the curve is $\int_\mathbb{R} R(t)dt = b$ and it is easily checked that the maximum value is $R_{max} = R\left(\frac{\beta-1}{\mu}\right) = b\frac{\mu^\beta}{\Gamma(\beta)}\left(\frac{\beta-1}{\mu}\right)^{\beta-1}e^{1-\beta}$. Calculating the ratio of σ_Γ and MTT_Γ from (12) leads to

$$\frac{\sigma_\Gamma}{MTT_\Gamma} = \frac{\sqrt{\beta}}{\Gamma(\beta)}\frac{(\beta-1)^{\beta-1}}{e^{\beta-1}}. \tag{16}$$

This expression depends on parameter β only. Figure 6 shows this function in dependence on β. The dashed horizontal line indicates the asymptotic value of the function as $\beta \to \infty$.
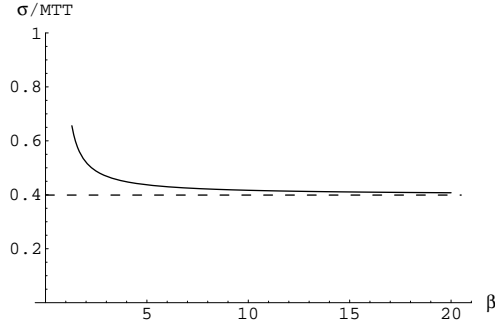

Figure 6: *Theoretical relation between σ and MTT in the case of a gamma density, in dependence on the parameter β. The dashed line runs at height $\frac{1}{\sqrt{2\pi}} \simeq 0.39$.*

Stirling's formula [1, Eq. 6.1.37] states that

$$\Gamma(x) = e^{-x}\,x^{x-\frac{1}{2}}\sqrt{2\pi}\,(1+\mathcal{O}(x^{-1})) \tag{17}$$

as $x \to \infty$. With this expression we get

$$\frac{\sigma_\Gamma}{MTT_\Gamma} = \frac{1}{\sqrt{2\pi}}\frac{\beta}{\beta-1} + \mathcal{O}(\beta^{-1}) \quad\xrightarrow{\beta\to\infty}\quad \frac{1}{\sqrt{2\pi}} \simeq 0.39\;. \tag{18}$$

Using the standard deviation of the IRF as a measure for the mean transit time, one gets significantly different values in dependence on the tissue type. Tissue with a permeable blood brain barrier (e.g., brain tumor) possesses a greater mean transit time than normal tissue (compare with figure 5 again).

To turn this into a practical method, the following ansatz looks promising. It is possible to determine the standard deviation of the IRF directly from the given (noisy) data without making an explicit deconvolution. Equation (2) implies $\sigma_{f*g}^2 = \sigma_f^2 + \sigma_g^2$, if f and g are probability densities. Consequently, the standard deviation of g can be calculated as

$$\sigma_g = \sqrt{\sigma_{f*g}^2 - \sigma_f^2}\;. \tag{19}$$

11

In our case, we have to normalize the signals prior to applying (19). This can be done on the basis of the discrete data directly. Our signals are available as a finite time series $\{h_\ell \mid 1 \leq \ell \leq n_{max}\}$, where we assume, for simplicity, that the integral index ℓ is the time (this being literally true for our MR test data). The normalization leads to

$$p_\ell = \frac{h_\ell}{\sum_j h_j} \ ,$$ (20)

where h_k are the non-normalized values of the respective signal and p_k the normalized ones. This way, one gets discrete probability distributions. Therefore, mean m and variance σ^2 read

$$m = \sum_\ell \ell p_\ell$$
$$\sigma^2 = \left(\sum_\ell \ell^2 p_\ell\right) - m^2 \ .$$ (21)

Using Eq. (19), the standard deviation of the IRF can now be computed.

Taking the values from the first pass of the signals (which refers to their structure in time, see [3]), the standard deviation provides already differences in dependence on the tissue type. We tested this with some exemplary patient data. For both MR and CT data, the values were between 1.8 and 2.6 in the case of normal tissue and between 3.1 and 3.4 in the case of a brain tumor. This way, getting a first indication in respect of the tissue type seems possible. Amazingly, such information can also be extracted from CT data, in spite of the rather short time series available.

5 Concluding remarks

Our brief exposition shows two things. First, a reasonable parametric description of blood flow data, both from MR and CT, is possible and does not suffer from standard problems of numerical deconvolution methods.

Second, the IRF is sufficiently accessible to draw first conclusions on the tissue type from it. In this context, we suggest the use of the standard deviation of the IRF as a potential diagnostic parameter.

All our methods were tested on real data, which are contained in [13]. However, this clearly needs further investigation, and a systematic test with a much larger data set. We hope to report on some progress in the near future.

Appendix: Positivity and positive definiteness

Let us explain the connection between these concepts, where we follow [4]. A complex-valued function φ on the real line is called *positive definite*, if for all $n \in \mathbb{N}$ and for all

n-tupels $(x_1, \ldots, x_n)$ with $x_i \in \mathbb{R}$, the $n{\times}n$ matrix $(\,\varphi(x_i{-}x_j)\,)_{1 \leq i,j \leq n}$ is positive Hermitian.

This definition implies the following properties:

(1) $\varphi(0) \geq 0$

(2) $\varphi(-x) = \overline{\varphi(x)}, \quad$ for all $x \in \mathbb{R}$

(3) $|\varphi(x)| \leq \varphi(0), \quad$ for all $x \in \mathbb{R}$

(4) $|\varphi(x) - \varphi(y)|^2 \leq 2\,\varphi(0)\,(\,\varphi(0) - \mathrm{Re}(\varphi(x-y))\,),$

see [4, Ch. 3.4] for details. Property (4) is often called Krein's inequality.

A function φ is positive definite if and only if there is a finite positive measure μ on $\mathbb{R}$ such that

$$\varphi(x) = \int_{\mathbb{R}} e^{ixy}\,d\mu(y)\ . \tag{22}$$

Moreover, φ is real-valued if the measure μ is symmetric, i.e., $\mu(A) = \mu(-A)$ for all Borel subsets of $\mathbb{R}$. This is a special case of Bochner's theorem, compare [4, Thm. 3.12], and μ is uniquely determined.

The special case that μ is a probability measure leads to $\varphi(0) = 1$. The function φ is now the characteristic function of μ, and the correspondence between positive definiteness of φ, with $\varphi(0) = 1$, and μ being a probability measure is also called the Bochner-Khintchine theorem [14].

In our case, the function φ is given and we need to know whether the corresponding μ, the IRF, is a positive signal function. The latter is a special case of a positive measure.

If, however, any of the properties (1) – (4) fails, we can conclude that μ cannot be a positive measure, and hence certainly not a positive signal.

Acknowledgements

References

[1] M. Abramowitz and I. A. Stegun, *Handbook of Mathematical Functions*, 10th ed., Dover, New York (1972).

[2] L. Axel, Tissue Mean Transit Time from Dynamic Computed Tomography by a Simple Deconvolution Technique, *Investigative Radiology* **18** (1983) 94–99.

[3] T. Benner, S. Heiland, G. Erb, M. Forsting, and K. Sartor, Accuracy of Gamma-Variate-Fits to Concentration-Time Curves from Dynamic Susceptibility-Contrast Enhanced MRI: Influence of Time Resolution, Maximal Signal Drop and Signal-To-Noise, *Magnetic Resonance Imaging* **15** (1997) 307–317.

[4] C. Berg and G. Forst, *Potential Theory on Locally Compact Abelian Groups*, Springer, Berlin (1975).

[5] A. Bock et al., Quantification of the Embolization Effect in Intracranial Meningeomas by $T2^*$–Weighted MR–Perfusion Measurement, *Klinische Neuroradiologie* **8** (1998) 30–41.

[6] R. N. Bracewell, *The Fourier Transform and Its Applications*, rev. 2nd ed., McGraw Hill, New York (1986).

[7] A. Cenic, D. G. Nabavi, R. A. Craen, A. W. Gelb and T. Y. Lee, Dynamic CT Measurement of Cerebral Blood Flow: A Validation Study, *American Journal of Neuroradiology* **20** (1999) 63–73.

[8] A. Cenic, D. G. Nabavi, R. A. Craen, A. W. Gelb and T. Y. Lee, A CT Method to Measure Hemodynamics in Brain Tumors: Validation and Application of Cerebral Blood Flow Maps, *American Journal of Neuroradiology* **21** (2000) 462–470.

[9] R. Durrett, *Probability*, Wadsworth, Belmont (1991).

[10] A. Erdélyi, *Tables of Integral Transforms*, vol. 1, McGraw Hill, New York (1954).

[11] I. I. Hirschman and D. V. Widder, *The Convolution Transform*, Princeton University Press, Princeton (1955).

[12] M. Kendall and A. Stuart, *Advanced Theory of Statistics*, vol. 1, 5th ed., Charles Griffin & Co, London (1987).

[13] E. Rost, *Signalanalyse und Entfaltungsverfahren für Kontrastmitteluntersuchungen mittels Schnittbildverfahren*, diploma thesis, Universität Greifswald (2005).

[14] A. N. Shiryayev, *Probability*, 2nd ed., Springer, New York (1996).

[15] D. Stark and W. Bradley, *Magnetic Resonance Imaging*, 3rd ed., Elsevier Books, Oxford (1998).

[16] J. K. Tajik, B. Q. Tran and E. A. Hoffmann, New Technique to Quantitate Regional Pulmonary Microvascular Transit Times from Dynamic X-ray CT Images, in: Proceedings of the Pacific Medical Technology Symposium (1998), R. Nelson, A. Gelish and S. K. Mun (eds.), available online[1].

[17] R. Wirestam, L. Andersson, L. Østergaard, M. Bolling, J.-P. Aunola, A. Lindgren, B. Geijer, S. Holtås and F. Ståhlberg, Assessment of Regional Cerebral Blood Flow by Dynamic Susceptibility Contrast MRI Using Different Deconvolution Techniques, *Magnetic Resonance in Medicine* **43** (2000) 691–700.

---

[1]available at: http://csdl.computer.org/comp/proceedings/pacmedtek/1998/8667/00/8667toc.htm.